Elsevier Editorial System(tm) for Geomorphology

Manuscript Draft

Manuscript Number: GEOMOR-6262

Title: Sediment mobility and velocity in a glacier-fed stream

Article Type: Special Issue: SEDALP

Keywords: PIT tags
Stationary antennas
Virtual velocity
Antecedent flows
Glacial regime
Alps

Corresponding Author: Prof. luca mao,

Corresponding Author's Institution: Pontificia Universidad Catolica de Chile

First Author: luca mao

Order of Authors: luca mao; Andrea Dell'Agnese; Francesco Comiti

Abstract: RFID passive integrated transponders (PIT) have become a popular method to investigate bedload dynamics at the particle scale in the river channel network, with PIT-tagged clasts usually located after bedload events by means of portable antennas. Stationary PIT antennas have been scarcely deployed so far, probably for technical constraints, despite they present the great advantage to identify the actual discharge at the moment of sediment motion. This study focuses on incipient motion of tracers measured by means of a stationary antennas system in a steep mountain channel (Saldur River, drainage area 18.6 km2, Italian Alps) where significant daily discharge fluctuations and bedload transport occur as a result of its nivo-glacial regime. A total of 629 PIT-tagged clasts were inserted in study reach in the period 2011-2014, ranging in size from 35 mm to 580 mm. Results show that the relationship between the size of transported tracers and the discharge measured at the time clasts were passing past the stationary antenna is weak. Hence, the influence of antecedent flows on incipient motion was investigated by dividing the peak discharge recorded between each PIT deployment and the subsequent entrainment by the actual critical discharge at the time of movement (ratio Qmax/Qc). Results show that only 35% of tracers moved at Qmax/Qc ≤ 1.1, and that 70% of tracers moved at Qmax/Qc < 1.5. Therefore, about 30% of tracers had to previously experience a discharge substantially higher than the one which actually mobilized them. Also, coarser particles moved at higher Qmax/Qc ratios, suggesting that higher antecedent flows may be needed for destabilizing the bed clustering. Virtual velocity of PIT-tagged clasts turned out to be highly variable and weakly related with both particle size and flow discharge. However, a better relationships exists between the virtual velocity and the ratio between the maximum discharge experienced by a clast and the difference between this and a percentile of the flow duration curve. This evidence further stresses the importance of flow history on sediment entrainment and transport.

Suggested Reviewers: Kristin Bunte
Colorado State University
kbunte@engr.colostate.edu

Marwan Hassan
The University of British Columbia
marwan.hassan@geog.ubc.ca

Bruce MacVicar
University of Waterloo
bmacvica@uwaterloo.ca

Sediment mobility and velocity in a glacier-fed stream

Mao L.[1*], Dell'Agnese A.[2], Comiti F.[2]

[1] Pontificia Universidad Católica de Chile, Department of Ecosystems and Environments, Santiago, Chile

[2] Faculty of Science and Technology, Free University of Bolzano, Bozen-Bolzano, Italy

* Correspondence to: Luca Mao, Department of Ecosystems and Environments, Pontificia Universidad Católica de Chile, Av. Vicuña Mackenna 4860, Macul, Santiago, Chile. Email: lmao@uc.cl

Abstract

RFID passive integrated transponders (PIT) have become a popular method to investigate bedload dynamics at the particle scale in the river channel network, with PIT-tagged clasts usually located after bedload events by means of portable antennas. Stationary PIT antennas have been scarcely deployed so far, probably for technical constraints, despite they present the great advantage to identify the actual discharge at the moment of sediment motion. This study focuses on incipient motion of tracers measured by means of a stationary antennas system in a steep mountain channel (Saldur River, drainage area 18.6 km^2, Italian Alps) where significant daily discharge fluctuations and bedload transport occur as a result of its nivo-glacial regime. A total of 629 PIT-tagged clasts were inserted in study reach in the period 2011-2014, ranging in size from 35 mm to 580 mm. Results show that the relationship between the size of transported tracers and the discharge measured at the time clasts were passing past the stationary antenna is weak. Hence, the influence of antecedent flows on incipient motion was investigated by dividing the peak discharge recorded between each PIT deployment and the subsequent entrainment by the actual critical discharge at the time of movement (ratio Q_{max}/Q_c). Results show that only 35% of tracers moved at $Q_{max}/Q_c \leq 1.1$, and that 70% of tracers moved at $Q_{max}/Q_c < 1.5$. Therefore, about 30% of tracers had to previously experience a discharge substantially higher than the one which actually mobilized them. Also, coarser particles moved at higher Q_{max}/Q_c ratios, suggesting that higher antecedent flows may be needed for destabilizing the bed clustering. Virtual velocity of PIT-tagged clasts turned out to be highly variable and weakly related with both particle size and flow discharge. However, a better relationships exists between the virtual velocity and the ratio between the maximum discharge experienced by a clast and the difference between this and a percentile of the flow duration curve. This evidence further stresses the importance of flow history on sediment entrainment and transport.

Keywords: PIT tag; Stationary antennas; Virtual velocity; Antecedent flows; Glacial regime; Alps

Introduction

The evaluation and prediction of coarse sediment movement and transport is crucial for understanding and prediction of fluvial morphodynamics, for designing flood hazard mitigation structures, and stream habitat restoration. However, bedload is notoriously challenging to measure in the field with samplers (e.g Vericat et al., 2006), and difficult to predict within one to two orders of magnitude using available formulas, especially in mountain rivers (e.g. Barry et al., 2004; Recking et al., 2012). Indeed, bedload equations are usually empirical and derived from data acquired through flume experiments (e.g. Wilcock & Crowe, 2003), when simplifications are made regarding the size and rate of sediment supply (Parker & Wilcock, 1993), the hysteresis of bedload transport (Mao, 2012; Mao et al., 2014), and the presence of armor layer (Mao et al., 2011).

Almost all of the existing sediment transport formulas contain a grain size-related threshold to predict the sediment incipient motion. A plethora of sediment entrainment methods and formulas have been proposed, but none of these give consistent answers even when they are applied to apparently similar conditions. This is evident from the work of Buffington & Montgomery (1997) who reported an order of magnitude difference (0.015 to 0.10) in the calculated dimensionless critical shear stress (Shields parameter). This is in part due to the subjectivity in defining threshold conditions (Buffington & Montgomery, 1997), but mainly due to relative submergence effect (e.g. Shvidchenko & Pender, 2000), and to the sensitivity of threshold entrainment to grain protrusion and local turbulent fluctuations (e.g. Lamb et al., 2008). In steep mountain rivers, the variability in incipient motion threshold is even more pronounced (Lenzi et al., 2006a; Bunte et al., 2013)

A further factor strongly influencing incipient motion - almost neglected until a decade ago is the range of flows lower than the critical threshold for grain incipient motion under which a channel bed is exposed prior to the movement of particles. Monteith & Pender (2005) and Haynes & Pender (2007) reported that higher antecedent shear stresses reduce bed stability due to the selective entrainment of the fine matrix within the bed. Piedra et al. (2012) explored this very process in flume experiments in a gravel bed, and highlighted the role of coarse-grain clusters in stabilizing the bed surface. Curran & Waters (2014) further observed that the percentage of sand on the channel bed can also exert a strong influence over the change in surface roughness and structure during armouring developed under rising flow rates.

All the above highlights the fact that the antecedent flows can have a strong influence on the dynamics of sediment transport, and that there is the need of exploring the effects of previous flows on sediment entrainment. However, because it is difficult to identify and monitor thresholds for sediment entrainment in mountain streams with traditional methods (i.e. competence calculations using data provided by samplers, e.g. Andrews, 1983), advanced studies involving the use of Passive Integrated Transponders (PIT) tags have increasingly being used over the last decade. PIT tags are encrypted with unique identification code and, inserted in individual grains, they can be used to track coarse particle movement in streams, allowing the measurement of displacement distances, thickness of active sediment layer, and development and maintenance of sediment structures and bedforms (e.g. Lamarre et al., 2005; Houbrechts et al., 2012; Bradley & Tucker, 2012; Chapuis et al., 2014, 2015; Phillips & Jerolmack, 2014; Dell'Agnese et al., 2015). PITs are not equipped with a battery and rely on an external power source, delivered by the reader through an antenna. The antenna is usually connected to a portable reader, thus PITs are searched for on the channel bed after floods. However, stationary antennas fixed on the channel bed have the potential to identify the actual discharge at the time of transport, and dynamics of sediment movement during floods. Using motion-sensing radio transmitters implanted in sediments and two stationary receiving stations, May & Pryor (2014) determined that the sequence of flood events and the history of under-threshold flows may be important to determine surface bed structures and sediment mobility.

Stationary antennas and PIT tags can also provide crucial information on velocity of sediments, which can be used to calculate bedload transport rates. In fact, the so-called virtual velocity approach involves the estimate of the virtual velocity of particle movement, the thickness of the active layer, and the active width of the streambed for calculating the rate of transport of bed material (Haschenburger & Church, 1998; Liebault & Laronne, 2008). The velocity of particle movement is considered “virtual” because it is generally calculated using the displacement of tracers and the interval between two subsequent surveys in the field. Even if one consider only over-threshold flows occurred between the two surveys (e.g. Dell’Agnese et al., 2015), by incorporating theoretical periods of both particles motion and rest, the calculated velocity tends to be less than the actual velocity during particle movements.

This paper presents a field investigation on bedload mobility and virtual velocities by stationary antennas and PIT-tagged clasts in a steep mountain river (Saldur River) of the Italian Alps, which is characterized by frequent bedload events due to its nivo-glacial hydrological regime. The objectives of the paper are to i) determine how strong is the relation between flow discharge and the size of transported sediments in steep channels (typically characterized by supply-limited conditions); ii) verify the extent to which antecedent flow conditions play a role on motion threshold discharges; iii) determine how virtual velocities vary with sediment size and flow conditions.

Methods

The study area is the upper Saldur basin (18.6 km^2 in drainage area, located in the Eastern Italian Alps), which ranges in elevation from 2150 m a.s.l. (bedload monitoring site, LSG in Figure 1) and 3738 m a.s.l. (Weisskugel/Palla Bianca peak), and features a metamorphic substrate mostly composed of orthogneiss (Habler et al., 2009). The catchment was entirely glaciated during the Pleistocene, whereas now only a small glacier (2.3 km^2 in 2013) is present in its upper part. The land use is characterized by alpine shrubs and grasslands up to 2700 m. a.s.l. and 2400 m. a.s.l on south and north faced slopes, respectively. The mean annual precipitation is estimated to range approximately from 800 mm in the lower part to 1500 mm in its upper portion, where 80% falls as snow (Penna et al., in review). Precipitation occurs as snowfall from November to late April, but snow storms often take place also during the summer at the higher elevations. The relatively low amount of liquid precipitation, a complete snow cover lasting until late April-late, and the presence of the glacier determine a characteristic nivo-glacial regime in the main Saldur River (Penna et al., 2014), where melt flows dominate the annual water budget. Snowmelt dominates from June to mid-July, when glacier melt takes over lasting until September or even later (Engel et al., in press; Penna et al., in review).

The longitudinal profile of the river displays a series of valley steps, the largest and steepest of which are in bedrock, the others due to the alluvial fans built by the tributaries (Mao et al., 2014). The average channel slope is 12.6%. The reach just upstream of the monitoring station is confined by the adjacent hillslopes and features a 6% slope, 5-6 m width, and a bed morphology transitional from plane-bed to step-pool. Surface grain size distribution is characterized here by the following percentiles (in mm): D_{16} = 43, D_{50} =108, D_{84} = 304, and D_{90} = 417. Subsurface sediments – sampled after removing the surface layer – are finer (D_{50} and D_{84} equal to 15 and 46 mm, respectively). More details on the Saldur channel morphology are given in Mao et al. (2014).

The monitoring station at 2150 m a.s.l. was installed in May-June 2011 and includes: i) a pressure transducer to record flow stage at 10 min intervals (flow rating curves were obtained by 82 salt dilution discharge measurements taken under different flow conditions between 2011 and

2014; ii) a 0.5m long acoustic pipe sensor, manufactured by Hydrotech Company (Japan), the same measuring instrument deployed in several Japanese streams since the 1990s (Mizuyama et al., 2010); iii) four stationary antennas for Passive Integrated Transponders (PIT), controlled by a specific module with datalogger manufactured by the company Aquartis (Canada), originally developed for fish monitoring. An interesting, seasonally-varying bedload dynamics – characterized by marked differences in the flow-bedload relationship between snowmelt and glacier melt periods – was inferred through the continuous records of the pipe sensor, and described in Mao et al. (2014). The calibration of the acoustic sensor through bedload samples – collected using portable bedload traps – was instead presented by Dell'Agnese et al. (2014).

This paper focuses only on the data gained from the combined use of PIT-tagged clasts and the stationary antennas to detect their passage at given sections, which offer valuable insights into bedload mobility and virtual velocity in steep channels. A stationary antennas for PIT tags is essentially a loop of normal electrical wire, spanning the entire width of the channel. Four of these electrical circuits were connected to the Aquartis controlling module "Quatro", which was powered by two car-size batteries (6V and 240Ah each), charged by a large solar panel (110 Watt). All these components were hosted on an electrical box installed near the bank of the Saldur channel (Figure 2a). The system registers on a SD card the time of passage (at 1 s resolution) of PIT-tagged clasts above/below the antennas, along with PIT identification number and the number of the detecting antenna (1 to 4, labelled from upstream to downstream in our case).

One antenna (antenna 4, the most downstream one) could be firmly installed on the stream bed (wires were first protected by PVC pipes and junctions, to create a rectangular semi-rigid frame) in close proximity of the acoustic pipe sensor (Figure 2b), thanks to the availability – at the section only – of an excavator which could fix the plastic frame by placing large flat boulders on it. Additional metal braces secured the lateral sides of the frame to the banks. The other 3 antennas were initially installed on the bed in the upstream reach (spaced approximately 50 m apart, covering a 150m-long reach) by hammering long, U-shaped rebars into the bed. Unfortunately, these were not able to keep the antennas at place once bedload initiated. Therefore, the three upper antennas were then placed above the channel (at about the bankfull stage elevation), without the PVC frame, fixing them by ropes and steel nails on the banks (Figure 2c). The vertical detection range was set to the maximum achievable with the available power supply, and varied between 0.5 m and 0.7 m in the different antennas, and such values were sufficient to detect PIT passages from the suspended antennas in the shallow Saldur flows. Figure 3 shows the lower part of the monitored reach, between antenna number 4 and antenna number 3.

The system was kept operational from June to September in the years 2011-2014, as the suspended antennas – as well as the batteries – were removed in early fall and reinstalled in late spring. Antenna 4, the only one secured at the streambed, provided the most continuous records of PIT passages from 2011 to 2014, as the others required maintenance after high flows due to small bank erosions and direct damages to the wires caused by the fast flows, and therefore for some periods they were not properly functioning. Antenna 1, the most upstream one and located in the least favorable section (easily erodible banks), functioned for the shortest time and could not detect any particles passage.

A total of 629 PIT-tagged clasts were inserted in study reach in the period 2011-2014, ranging in size (b-axis diameter) from 35 mm to 580 mm. Only natural clasts present in the Saldur channel were equipped with PIT tags (standard, 23 mm-long) directly in the field, by i) drilling holes 5 mm in diameter; ii) inserting a PIT in the hole; iii) applying a water-resistance glue; iv) leaving the glue to dry out for about a day. The three diameters of each tagged particles were then measured by a digital caliper for the smaller sizes and by a tree caliper for the larger clasts. 417 clasts were also weighed by a digital scale in the field, in order to determine the relationship between b-axis diameter and weight, and to test whether the use of particle weight brings about better statistical relationships, as found by Dell'Agnese et al. (2015).

Once tagged clasts were ready, they were placed on the bed surface at different positions, immediately upstream of the antennas, and their longitudinal distance from each antenna was noted. An exception were 50 tagged particles (60 mm – 300 mm in diameter) which were laid 2 km upstream from the bedload monitoring station (near the weather station marked as WS in Figure 1) in 2012. These additional clasts were inserted to determine how virtual velocity (in case of their detection by the stationary antennas) can be affected by the spatial scale of transport. At the end of each summer season, until October 2013, the location of PIT-tagged clasts remained within the study reach (i.e. only between antenna 1 and 4) was detected by a portable PIT antenna, the same used in a different stream by Dell'Agnese et al (2015). For logistical reasons (inaccessibility of the site) these surveys could not be performed at the end of the summer 2014.

Results and discussion

General observations

During the 2011-2014 period, 275 particles were detected by at least one antenna, 24 were detected by two antennas, and only 2 by three antennas. None was detected by all the four antennas, also because – as mentioned above – the upstream-most one (antenna 1) could be operational for a very short period due to the unstable banks of that cross-section. The range of detected particle size is from 40 mm to 450 mm (0.1 kg – 78 kg), thus spanning almost entirely the size range laid on the bed. Indeed, the grain size distribution of the detected particles is almost identical to the one of the entire tagged dataset (Figure 4).

At the end of summer 2013, 103 tagged clasts were found – thanks to the portable PIT antenna – to be still within the study reach, indicating that, in the period 2011-2013, 236 clasts became either deeply buried in the bed and thus not detectable or were transported downstream of Antenna 4 without being "caught" by the system. We think the latter hypothesis is more likely, because i) relevant bed changes were not evident in the Saldur River by performing repeated cross-section surveys and visual observation of the streambed; and ii) the PIT system was – for some days – made "blind" by tagged clasts which stopped below the antennas, preventing the acquisition system to read other possible PIT passages below the other antennas until the "disturbing" particle was removed. As already said, multiples passages of the same clast below two different antennas were 24, and most of them derives from signals at antenna 2 and 4. In these cases the time interval between the two consecutive passages ranged from 1 min to 10 hr, on average 2 hr. This means that some particles already in motion below antenna 2 could travel to antenna 4 (106 m downstream) within the time of daily bedload transporting events associated to snow- and glacier melt runoff, which typically last – based on the acoustic pipe signal – from 12-14 hours (during late summer glacier melt) to the entire day (hot spells during snowmelt). On the other hand, 22 tagged particles passed below antenna 2 and were not either detected by antenna 3 or 4 or found by the mobile antenna. Details on melt flow hydrographs in the Saldur River during the study period are given in Engel et al. (in press). The analysis of particle velocities will presented later.

Remarkably, none of the tagged particles placed at the end of July 2012 about 2 km upstream of the monitoring station was detected by the antennas. Unfortunately, for the reasons just mentioned, we could not achieve a 100% detection range in our monitored reach, and thus we cannot actually claim with certainty that these tagged clasts did not travel down to the antennas by the end of 2014. However, it seems likely that many – if not most – of the clasts inserted 2 km upstream of the station were not transported for such a distance within the monitored period. This hypothesis would match the lowest values of virtual velocities – determined from the placement time to the detection time – observed for the tagged particles within the study reach (see later).

Critical discharge for motion and antecedent flows

Figure 5 shows that the grain size of the transported sediments – detected by at least one antenna – is only weekly correlated with the flow discharge at the time of their passage past the stationary antennas ($r = 0.19$, $p < 0.05$), also considering the upper boundary of the scatterplot only. Such pattern is not substantially modified when adopting the particle weight instead of the b-axis of the clasts, and thus we prefer to analyze transported particles in terms of grain size, as usually done (but differently from Dell'Agnese et al., 2015, in a stream where probably more irregularly shaped clasts made the use of weight beneficial). In more detail, Figure 5 shows that tracers of around 100 mm (corresponding to the D_{50} of the bed surface) were transported even at very low discharges (1.4 $m^3 s^{-1}$), very close to the bedload motion threshold (as determined by Dell'Agnese et al. 2014 by direct bedload sampling). The largest measured flow rate in the study period (14.3 $m^3 s^{-1}$) mobilized tagged clasts up to 300 mm, but the largest tagged particle (450 mm, corresponding to about the D_{90} of the bed surface) was transported by a discharge of approximately 3 $m^3 s^{-1}$, that is lower than the bankfull stage (estimated in the study reach to be between 4 and 4.5 $m^3 s^{-1}$, Dell'Agnese et al., 2014). On the other hand, visual observations of the channel bed indicated that (non-tagged) clasts up to 0.7 – 0.8 m were mobilized by the largest flows (10-15 $m^3 s^{-1}$) associated to rainstorms, which anyhow cannot be considered as infrequent floods based on regional values of specific discharges. Unfortunately, a reliable magnitude-frequency relationship cannot be obtained due to the short time series available so far. Nonetheless, the mobility of the bed sediments in the Saldur River seems overall much more pronounced than in other steep channels (Lenzi et al., 2006a; Bunte et al., 2013) characterized by a different, non-glacial hydrological regime. In fact, Lenzi et al. (2006b) showed that the entrainment discharge for the D_{90}D84 of the channel bed in the Rio Cordon (a high-gradient stream of the Italian Alps) needed a discharge much more infrequent than the bankfull (i.e. 4.55 $m^3 s^{-1}$, with a recurrence interval of 4.2 years). The fact that the discharge is not a good predictor of the grain size of transported sediments can suggest the lack of size-selectivity. As originally formulated by Parker et al. (1982), strong hiding/protrusion effects can lead the same value of discharge or dimensional shear stress to be critical for all particle sizes, i.e. small and large clasts are entrained under the same flow rate, a conditions known as equimobility. Near-equimobility conditions have been identified by many authors (e.g. Andrews, 1983; Church et al., 1991; Batalla & Martin-Vide, 2001), although in other high-gradient streams a certain degree size-selective transport have also been reported (e.g Marion & Weirich, 2003; Carling, 1983; Lenzi et al., 2006a). However, the lack of a strong correlation between discharge and transported grain size (evident also by the results of the bedload sampling carried out by Dell'Agnese et al., 2014) might not be due to hiding/protrusion effects alone, but also to the fact that the discharge at the time of PIT's passages past the stationary antennas is not necessarily the only predictor of critical conditions for sediment entrainment.

The availability of flow discharges monitored between the placement of each tracer on the channel bed and its passage by the stationary antennas allows us to consider the magnitude of discharges occurred before the actual motion of the tracers. In particular, the influence of antecedent flows on incipient motion was investigated using the ratio between the maximum discharge recorded between each PIT deployment and the subsequent entrainment, and the actual "critical" discharge at the time of movement (i.e. the Q_{max}/Q_c ratio). The conceptual illustration of Figure 6 shows how the Q_{max}/Q_c ratio can be considered in a system characterized by daily fluctuation of discharges due to snow and glacier melting as is the Saldur River. If a conceptual sequence of flood events is considered, a tracer is entrained at a ratio Q_{max}/Q_c equal to one if no flows higher than the critical discharge for entrainment were experienced before the displacement (continuous line in Figure 6). Conversely, the larger the flow occurred before the actual entrainment, the higher the Q_{max}/Q_c ratio.

Figure 7 shows only 35% of tracers moved at $Q_{max}/Q_c \leq 1.1$, and that 70% of tracers moved at $Q_{max}/Q_c < 1.5$. Therefore, about 30% of tracers had to previously experience a discharge substantially higher than the one which actually mobilized them. In fact, 23.5% of tracers (i.e. 36 PITs) experienced a flow double than the value of the critical discharge (i.e. $Q_{max}/Q_c > 2$), and 2.5 % of tracers moved at a discharge than was previously exceeded by 3 times (i.e. $Q_{max}/Q_c > 3$). Interestingly, coarser particles tended to move at higher Q_{max}/Q_c ratios (Figure 8). For instance, 88 % of tracers finer than 45 mm moved at $Q_{max}/Q_c < 1.5$, whereas only 60 % of particles coarser than 256 mm moved with such small Q_{max}/Q_c ratio. On the other hand, no tracers finer than 45 mm moved at $Q_{max}/Q_c > 2$, but 20 % of particles coarser than 256 mm needed to experience a flow twice the critical discharge before being entrained.

This evidence suggests that higher antecedent flows may be needed for destabilizing the bed before particles can be entrained. In fact, early field works from the 1980s began to show that bedload transport showed hysteresis during floods, implying different conditions for sediment entrainment or supply during events. Klingeman & Emmett (1982) reported that the critical shear stress for incipient motion was greater in the rising limb of a flood due to the enhanced bed stability produced from the development of an amour layer. Later, Frostick et al. (1984) were the first to suggest that antecedent flows may control the proportion of matrix fines in the bed and to explain why entrainment thresholds vary for individual flood events. Frostick et al. (2006) further showed using flume experiments that the infiltration of fine sediments into a gravel bed during high flows causes the dilatation of the gravel matrix. More recently, in analyzing bedload dynamics of a small gravel-bed river of Canada, Marquis & Roy (2012) discovered that morphological channel changes were not necessarily related with the mobility of sediment surfaces, leading to the identification of processes of bed dilation (due to fine sediment infiltration) and contraction (due to sediment winnowing) that occurred on the surface sediments. Marquis & Roy (2012) related the processes of bed dilation/contraction to the bed conditions left by the antecedent event, explicitly highlighting the role of previous floods on sediment transport and morphological changes in gravel-bed rivers. Furthermore, by flume experiments, Mao (2012) and Water & Curran (2015) showed that sediment transport hysteresis during floods is due to surface structure adjustments.

The evidence provided by the tagged particles in the Saldur River adds to these findings, shedding further light on the important role of flow history on sediment entrainment. In particular, high antecedent flows seem to favour mostly the transport of the coarser particles composing the bed. In the Saldur River the role of fine sediments cannot be assessed from the available data. However, even if dilation/contraction due to fine sediments infiltration and winnowing cannot be discarded, it seems more likely that the need of higher discharges before the actual entrainment could be related with the bed destabilization at the scale of sediment clusters taking place during the antecedent high flows. Destruction of morphological units (steps) were instead not observed during the monitoring period.

Virtual velocity of tracers

The virtual velocity of each particle was calculated either i) by knowing the time interval between the passage of the same clast by two antennas, and the distance among them (for the cases of multiple detection only, see above); or ii) by knowing the distance (ranging from 1 to 15 m) at which tagged particle were laid upstream of each antenna and the duration of over-threshold flows between their placement and detection by one antenna (for all the detected clasts). Even if here the velocity is calculated using the actual time of travel between two fixed points rather than the positions at which particles are found on two successive search (as usually done if only portable antennas are used), we call it virtual velocity as particles can clearly experience moments of movement and rest between antennas.

Figure 9a shows the relationships between virtual velocity and the size of tagged particles. It appears that the two variables are negatively but vert weakly correlated (r = -0.04), and that velocities measured on different sub-reaches (i.e. segments between antennas) appears to be comparable. Indeed, the data is very scattered, as the virtual velocity can vary among more than 5 orders of magnitude for particles finer than 200 mm. This was somehow expected, as sub-reaches can be 30 to 70 m long, and particles can rest on sediment clusters and bedforms as rapid, steps, and pools, which are found in the study site. The maximum measured virtual velocity is 35 m min^{-1} (i.e. 0.59 m s^{-1}), which is reasonable, as reach-averaged flow velocity during discharges of around 2.5 m^3 s^{-1} – at which the particle moved – is approximately 1.2 - 1.3 m s^{-1} (determined based on flow continuity principle and measured discharges at LSG). If one plots a curve enveloping the higher measured velocity, the regression would be $VV = 200e^{-0.03D}$, which could help determine the maximum virtual velocity (VV, in m min^{-1}) of sediments of different diameter (D, in mm) in a reach with the slope and morphological characteristics similar to the Saldur River. Interestingly, this upper envelope is similar to what proposed by Liebault et al. (2012) who traced PIT tags over long distances using a portable antenna in a wider (24 m) and gentler sloped (0.016 m m^{-1}) stream of the French Alps. The exponential decrease of virtual velocity with grain size reported by Liebault et al. (2012) showed a strong decrease in mobility for sediments coarser than 4 times the D_{50} of the bed surface. In the case of the Saldur River, this strong decrease appears to occur at a gran size about the double of the surface D_{50}, closer to what reported by Church & Hassan (1992) as a threshold for a rapid decline in grain mobility with increasing grain-size. The observed decrease of virtual velocity for coarser particles agree with findings of Ferguson & Wathen (1998) using tracers in a small stream of the Scottish Highlands, and with later investigations reported by Church & Hassan (2002), but not with more recent observations of Milan (2013) and Dell'Agnese et al. (2015) who calculated virtual velocity by dividing the displacement of tracers by the duration of competence time between two surveys. Instead, Liedermann et al. (2013) found decreasing transport distances with increasing tracer sizes in a large and regulated Austrian river (the Danube).

Figure 9b shows also the relationships between the virtual velocity and the maximum discharge. The two variables are weekly (R^2 = 0.184) and negatively correlated (r = -0.05). This is counterintuitive, as one would expect higher virtual velocities measured for intervals with larger discharges. Indeed, Ferguson & Wathen (1998) showed that virtual velocity tends to increase with shear stress. However, this could also suggest that the instantaneous maximum discharge experienced by a particles moving from one antenna to the following could not represent alone a good predictor for the virtual velocity, as also argued by Dell'Agnese et al. (2015).

Because the discharge was continuously measured along the monitoring seasons near the antenna 4 (LSG in Figure 1), the flow duration curve from the passage between the upper and lower antennas for each single particles have been calculated. Significant percentiles of the flow duration curves were calculated too. The better relationships have been found with a ratio between the maximum discharge and the difference between the maximum discharge and a percentile of the flow duration curve. Table 1 shows that the coefficients of determination are significantly higher (around 0.54) than using the Q^{max} alone, and that using percentiles closer to the maximum discharge seems to improve the performance of the empirical regression to predict the virtual velocity. Figure 10 shows the relationships between the virtual velocity and the $Q_{max}/(Q_{max}-Q_{10})$ ratio. Data plotted in the upper right portion of the graph represents particles that experienced higher maximum discharge but also long periods with high discharge (close to the maximum). Conversely, tracers that travelled with low virtual velocity experienced longer periods with lower discharge (e.g. late snow melting season). This suggests that the maximum discharge is not crucial in determining the virtual velocity of particles, at least during ordinary transport events results, and highlights the importance of magnitude and duration of antecedent flows. Among others, Hassan et al. (1992) and May & Pryor (2014) previously suggested that the magnitude of antecedent events has an influence on entrainment and displacement length or bed surface sediments. May & Pryor (2014) further observed that tracers moved preferably during the rising rather than the falling limbs of hydrographs, relating this with the dynamics of bed structures, as done before by Church & Hassan (1992) too.

Final remarks

This paper presents a novel set of evidence provided by a PIT-tagged experiment in a glacierized stream of the Italian Alps, where a 150-m long reach was instrumented with a set of 4 stationary antennas. Evidence shows that in this environment characterized by abrupt daily discharge fluctuations due to the nivo-glacial regime, the size of transported sediments is only weakly correlated with the discharge. The history of flows occurred before the actual movement of particles seems to play an important role on incipient motion in this environment, as 65% of PIT-tagged clasts experienced a discharge higher than the value of discharge at the time of entrainment (i.e. $Q_{max}/Q_c > 1.1$), and 30% of them moved at $Q_{max}/Q_c > 1.5$. Also, the virtual velocity of a PIT-tagged clasts resulted highly scattered and only weakly related with either particle size or the flow discharge. Again, including the flow history in the analysis by considering a ratio between the maximum discharge and the difference between this and a percentile of the flow duration curve proved to increase the significance of the relationship between the discharge and the virtual velocity of bed particles. Overall, this study highlights the important role of the magnitude and frequency of antecedent flows on sediment entrainment and displacement velocity in glacierized streams.

Acknowledgments

This research was funded by the projects "Effects of climate change on high-altitude ecosystems" (Free University of Bozen-Bolzano), "GESTO" (Aut. Province of Bozen-Bolzano), and "EMERGE: Retreating glaciers and emerging ecosystems in the Southern Alps" (Herzog-Sellenberg- und Ritter-Stiftung im Stifterverband für die DeutscheWissenschaft). During the research, LM was supported by an Incoming Researcher Fellowship provided by the Autonomous Province of Bozen-Bolzano while based at the Free University of Bozen-Bolzano. The Dept. of Hydraulic Engineering of the Aut. Province of Bolzano supported the installation of the monitoring system. Several collaborators helped in the field: Michael Engel, Ana Lucìa, Enrico Marchese, Joshua Theule, Enrico Buzzi, Alex Boninsegna, and Raffaele Foffa. Also, Normand Bergeron and Francis Berubé are thanked for helping with the installation of the stationary antenna system.

References

Andrews, E.D., 1983. Entrainment of gravel from naturally sorted riverbed material. Geological Society of American Bulletin 94, 1225–1231.

Barry, J.J., Buffington, J.M., King, J.G., 2004. A general power equation for predicting bedload transport rates in gravel bed rivers. Water Resour. Res. 40, W104001.

Batalla, R.J., Martin-Vide, J.P. 2001. Thresholds of particle entrainment in a poorly sorted sandy gravel-bed river. Catena 44, 223–243.

Bradley, D.N., Tucker, G.E., 2012. Measuring gravel transport and dispersion in a mountain river using passive radio tracers. Earth Surf. Proc. Land., 37, 1034–1045.

Buffington, J.M., Montgomery, D.R., 1997. A systematic analysis of eight decades of incipient motion studies, with special reference to gravel-bedded rivers. Water Resour. Res. 33, 1993-2029.

Bunte, K., Abt S.R., Swingle, K.W., Cenderelli, D.A., Schneider, J.M. (2013), Critical Shields values in coarse-bedded steep streams, Water Resour. Res. 49, 7427–7447.

Carling, P.A., 1983. Threshold of coarse sediment transport in broad and narrow natural streams. Earth Surface Processes and Landforms 8, 135–138.

Chapuis, M., Bright, C.J., Hufnagel, J., MacVicar B., 2014. Detection ranges and uncertainty of passive Radio Frequency Identification (RFID) transponders for sediment tracking in gravel rivers and coastal environments. Earth Surf. Process. Landf. 39, 2109-2120.

Chapuis, M., Dufour, S., Provansal, M., Couvert, B., de Linares, M., 2015. Coupling channel evolution monitoring and RFID tracking in a large, wandering, gravel-bed river: Insights into sediment routing on geomorphic continuity through a riffle–pool sequence. Geomorphology 231, 258-269.

Church, M., Hassan, M.A., 1992. Size and distance of travel of unconstrained clasts on a streambed. Water Resour. Res. 28(1), 299–303.

Church, M., Hassan, M.A., 2002. Mobility of bed material in Harris Creek. Water Resour. Res. 38(11), 1237.

Church, M., Wolcott, J.F., Fletcher, W.K., 1991. A test of equal mobility in fluvial sediment transport: behaviour of the sand fraction. Water Resour. Res. 27, 2941–2951.

Curran, J.C, Waters, K.A., 2014. The importance of bed sediment sand content for the structure of a static armor layer in a gravel bed river. Journal of Geophysical Research: Earth Surface 119, 1484–1497.

Dell'Agnese, A., Brardinoni, F., Toro, M., Mao, L., Engel, M., and Comiti, F., 2015. Bedload transport in a formerly glaciated mountain catchment constrained by particle tracking, Earth Surf. Dynam., 3, 527-542.

Dell'Agnese, A., Mao, L., Comiti, F., 2014. Calibration of an acoustic pipe sensor through bedload traps in a glacierized basin. Catena 121, 222-231.

Engel, M., Penna, D., Bertoldi, G., Dell'Agnese, A., Soulsby, C., Comiti, F., in press. Identifying run-off contributions during melt-induced run-off events in a glacierized alpine catchment. Hydrological Processes.

Ferguson, R.I., Wathen, S.J., 1998. Tracer-pebble movement along a concave river profile: virtual velocity in relation to grain size and shear stress. Water Resour. Res., 34, 2031–2038,

Frostick, L.E., Lucas, P.M., Reid, I., 1984. The infiltration of fine matrices into coarse-grained alluvial sediments and its implications for stratigraphical interpretation. Journal of Geological Society 141, 955-965.

Frostick, L.E., Murphy, B., Middleton, R., 2006. Unravelling flood history using matrices in fluvial gravel deposits. In Sediment Dynamics and the Hydromorphology of Fluvial Systems. IAHS 306, 425-433.

Habler, G., Thöni, M., Grasemann, B., 2009. Cretaceous metamorphism in the Austroalpine Matsch Unit (Eastern Alps): the interrelation between deformation and chemical equilibration processes. Miner. Petrol. 97, 149–171.

Haschenburger, J.K., Church, M., 1998. Bed material transport estimated from the virtual velocity of sediment. Earth Surf. Process. Landforms 23, 791–808.

Hassan, M.A., Church, M., Ashworth, P.J., 1992. Virtual rate and mean distance of travel of individual clasts in gravel bed channels. Earth Surf. Processes Landforms 17, 617-627.

Haynes, H., Pender, G., 2007. Stress history effects on graded bed stability. Journal of Hydraulic Engineering 133(4), 343-349.

Houbrechts, G., Van Campenhout, J., Levecq, Y., Hallot, E., Peeters, A., Petit, F., 2012. Comparison of methods for quantifying active layer dynamics and bedload discharge in armoured gravel-bed rivers. Earth Surf. Process. Landf. 37, 1501–1517.

Klingeman, P.C., Emmett, W.W., 1982. Gravel bedload transport processes. In: Gravel-Bed Rivers. Hey, R.D, Bathurst, J.C., Thorne, C. (eds), John Wiley, 141-169.

Lamarre, H., MacVicar, B., Roy, A.G., 2005. Using passive integrated transponder (PIT) tags to investigate sediment transport in gravel-bed rivers. Journal of Sedimentary Research 75(4), 736-741.

Lamb, M.P., Dietrich W.E., Venditti, J.G., 2008. Is the critical Shields stress for incipient sediment motion dependent on channel-bed slope? J. Geophys. Res. 113, F02008.

Lenzi, M.A., Mao, L., Comiti, F., 2006a. When does bedload transport begin in steep boulder-bed streams? Hydrological Processes 20, 3517-3533.

Lenzi, M.A., Mao, L., Comiti, F., 2006b. Effective discharge for sediment transport in a mountain river: Computational approaches and geomorphic effectiveness. Journal of Hydrology 326, 257–276.

Liébault, F., Bellot, H., Chapuis, M., Klotz, S., Deschâtres, M., 2012. Bedload tracing in a high-sediment-load mountain stream. Earth Surf. Process. Landforms 37, 385–399.

Liébault, F., Laronne, J., 2008. Evaluation of bedload yield in gravel-bed rivers using scour chains and painted tracers: the case of the Esconavette Torrent (Southern French Prealps). Geodinamica Acta 21(1-2), 23-34.

Liedermann, M., Tritthart, M. and Habersack, H., 2013. Particle path characteristics at the large gravel-bed river Danube: results from a tracer study and numerical modelling. Earth Surf. Process. Landforms 38, 512–522.

Mao, L., 2012. The effect of hydrographs on bed load transport and bed sediment spatial arrangement. Journal of Geophysical Research: Earth Surface 117, F03024.

Mao, L., Cooper, J.R., Frostick, L.E., 2011. Grain size and topographical differences between static and mobile armor layers. Earth Surf. Process. Landf. 36, 1321–1334.

Mao, L., Dell'Agnese, A., Huincache, C., Penna, D., Engel, M., Niedrist, G., Comiti, F., 2014. Bedload hysteresis in a glacier-fed mountain river. Earth Surf. Process. Landf. 39(7), 964-976.

Marion, D.A., Weirich, F., 2003. Equal-mobility bed load transport in a small, step–pool channel in the Ouachita Mountains. Geomorphology 55, 139–154.

Marquis, G.A., Roy, A.G., 2012. Using multiple bed load measurements: Toward the identification of bed dilation and contraction in gravel-bed rivers. Journal of Geophysical Research 117, F01014.

May, C.L., Pryor, B.S., 2014. Initial motion and bedload transport distance determined by particle tracking in a large regulated river. River Research and Applications 30(4), 508-520.

Milan, D.J.,2013. Virtual velocity of tracers in a gravel-bed river using size-based competence duration. Geomorphology 198, 107-114.

Mizuyama, T., Laronne, J.B., Nonaka, M., Sawada, T., Satofuka, Y., Matsuoka, M., Yamashita, S., Sako, Y., Tamaki, S., Watari, M., Yamaguchi, S., Tsuruta, K., 2010. Calibration of a passive acoustic bedload monitoring system in Japanese mountain rivers. U.S.G.S. Scientific Investigations Report 2010-5091.

Monteith, H., Pender, G., 2005. Flume investigations into the influence of shear stress history on a graded sediment bed. Water Resour. Res. 41, W12401,

Parker, G., Dhamotharan, S., Stefan, H., 1982. Model experiments on mobile, paved gravel bed streams. Water Resour. Res. 18(5), 1395–1408.

Parker, G., Wilcock, P.R., 1993. Sediment feed and recirculating flumes: A fundamental difference. Journal of Hydraulic Engineering 119(11), 1192–1204.

Penna, D., Engel, M., Bertoldi, G., Comiti, F., in review. Towards a tracer-based conceptualization of meltwater dynamics and streamflow response in a glacierized catchment. Submitted to Water Resour. Res.

Penna, D., Engel, M., Mao, L., Dell'Agnese, A., Bertoldi, G., Comiti, F., 2014. Tracer-based analysis of spatial and temporal variations of water sources in a glacierized catchment. Hydrology and Earth System Sciences 18, 5271–5288.

Phillips, C.B., Jerolmack, D.J., 2014. Dynamics and mechanics of bed load tracer particles. Earth Surface Dynamics Discussion, 2, 429-476.

Piedra, M.M., Haynes, H., Hoey, T.B., 2012. The spatial distribution of coarse surface grains and the stability of gravel river beds. Sedimentology 59, 1014–1029.

Recking, A., 2012. Influence of sediment supply on mountain streams bedload transport. Geomorphology 175-176, 139–150.

Shvidchenko, A.B., Pender, G., 2000. Flume study of the effect of relative depth on the incipient motion of coarse uniform sediments. Water Resour. Res. 36(2), 619–628.

Vericat, D., Church, M., Batalla, R.J., 2006. Bed load bias: Comparison of measurements obtained using two Helley-Smith samplers (76 and 152 mm) in a gravel-bed river. Water Resour. Res, 42, W01402.

Waters, K.A, Curran, J.C., 2015. Linking bed morphology changes of two sediment mixtures to sediment transport predictions in unsteady flows. Water Resour. Res. 51(4), 2724-2741.

Wilcock, P.R., Crowe, J.C., 2003. Surface-based transport model for mixed-size sediment. Journal of Hydraulic Engineering 129(2), 120–128.

Tables

Table 1. Coefficients, exponents, and coefficients of determination, for the power law regressions relating virtual velocity (VV in m min^{-1}) and a ratio between the maximum discharge and a significant percentile of the flow duration curve (numbers in bold are significant at p < 0.05).

	a	b	R^2
$VV = a\left(Q_{max}/(Q_{max} - Q_{50})\right)^b$	0.0003	**1.6332**	0.5413
$VV = a\left(Q_{max}/(Q_{max} - Q_{25})\right)^b$	0.0003	**1.3886**	0.5509
$VV = a\left(Q_{max}/(Q_{max} - Q_{10})\right)^b$	0.0002	**1.1777**	0.5517

Figure Caption

Figure 1. Location and map of the Saldur catchment showing the position of the monitoring station for bedload and water discharge (LSG). WS marks the location of the weather station managed by EURAC.

Figure 2. Case hosting the PIT detection system in the Saldur River (a), the antenna 4 being fixed in the channel bed at the downstream end of the study reach (b), and the antenna 2, placed above the channel after being damaged during a high flow, and detecting tagged particles passing below it.

Figure 3. A view of the Saldur River showing most of the study reach, with the location of the antenna's control unit and two antennas (3 and 4), placed 70 m apart. Antenna 2, not visible, is just behind the curve 36 m upstream of antenna 3.

Figure 4. Grain size distribution of the surface sediments, tagged particles and particles that were transported and detected by the stationary antennas.

Figure 5. Relationship between the intermediate diameter of the PITs and the discharge at the time of passage above an antenna.

Figure 6. Conceptual image showing an idealized sequence of flood events occurring after a PIT is placed in the channel bed. The largest the discharge occurred before the movement of the particle (thus the passage near an antenna), the higher the Q_{max}/Q_c ratio.

Figure 7. Frequency of Q_{max}/Q_c values experienced by the PIT tags monitored using the stationary antennas in the Saldur River.

Figure 8. Distribution of Q_{max}/Q_c ratios divided by grain size classes.

Figure 9. Relationships between the virtual velocity the size of PIT tags (on the left), and the discharge (on the right).

Figure 10. Relationship between the ratio of maximum discharge and the ratio between the maximum discharge and the percentile 10 of the flow duration curve (i.e. the discharge exceeded for 10% of the time in the flow duration curve) and the virtual velocity of tagged particles.

Figure (Color)

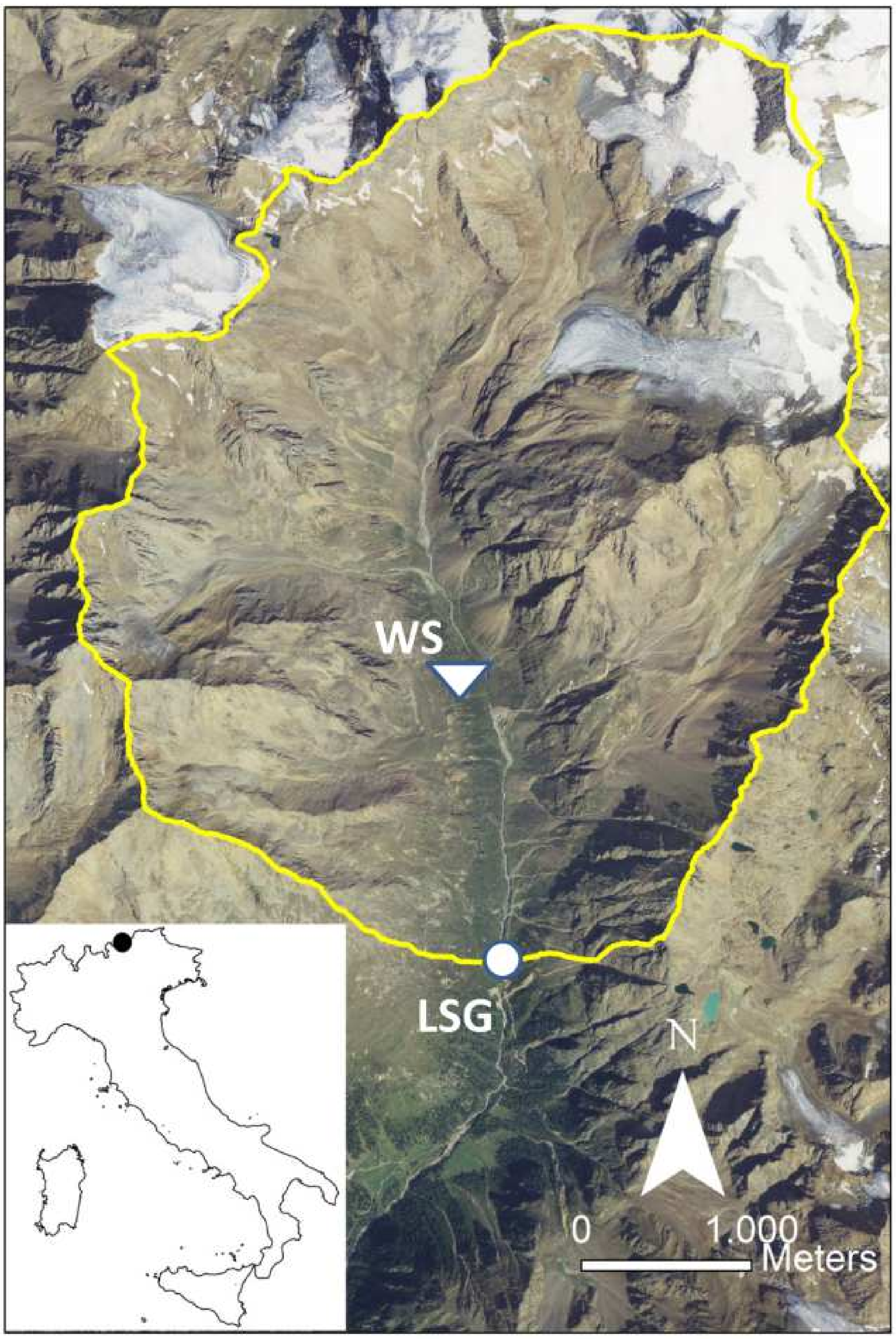

Figure (Greyscale)

Figure (Greyscale)

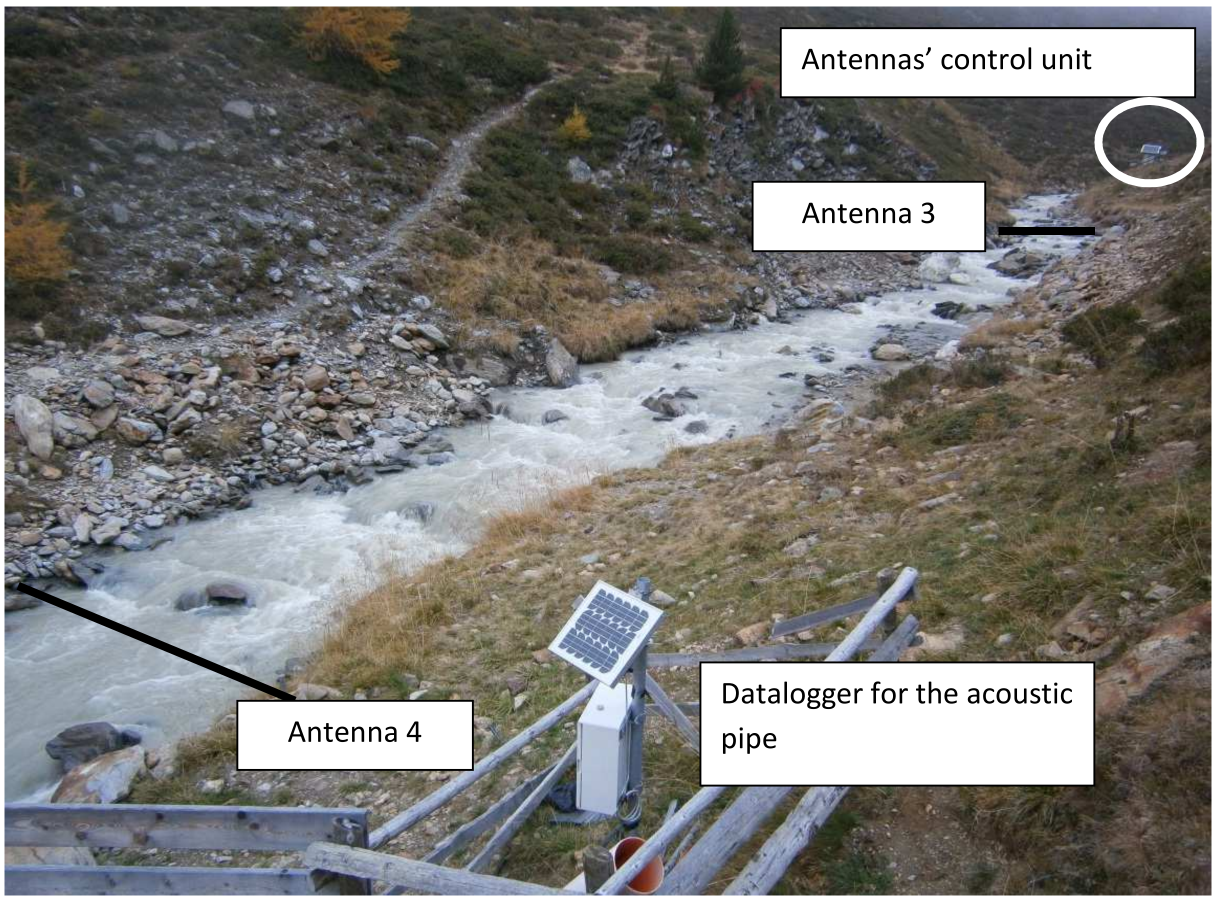

Figure (Greyscale)

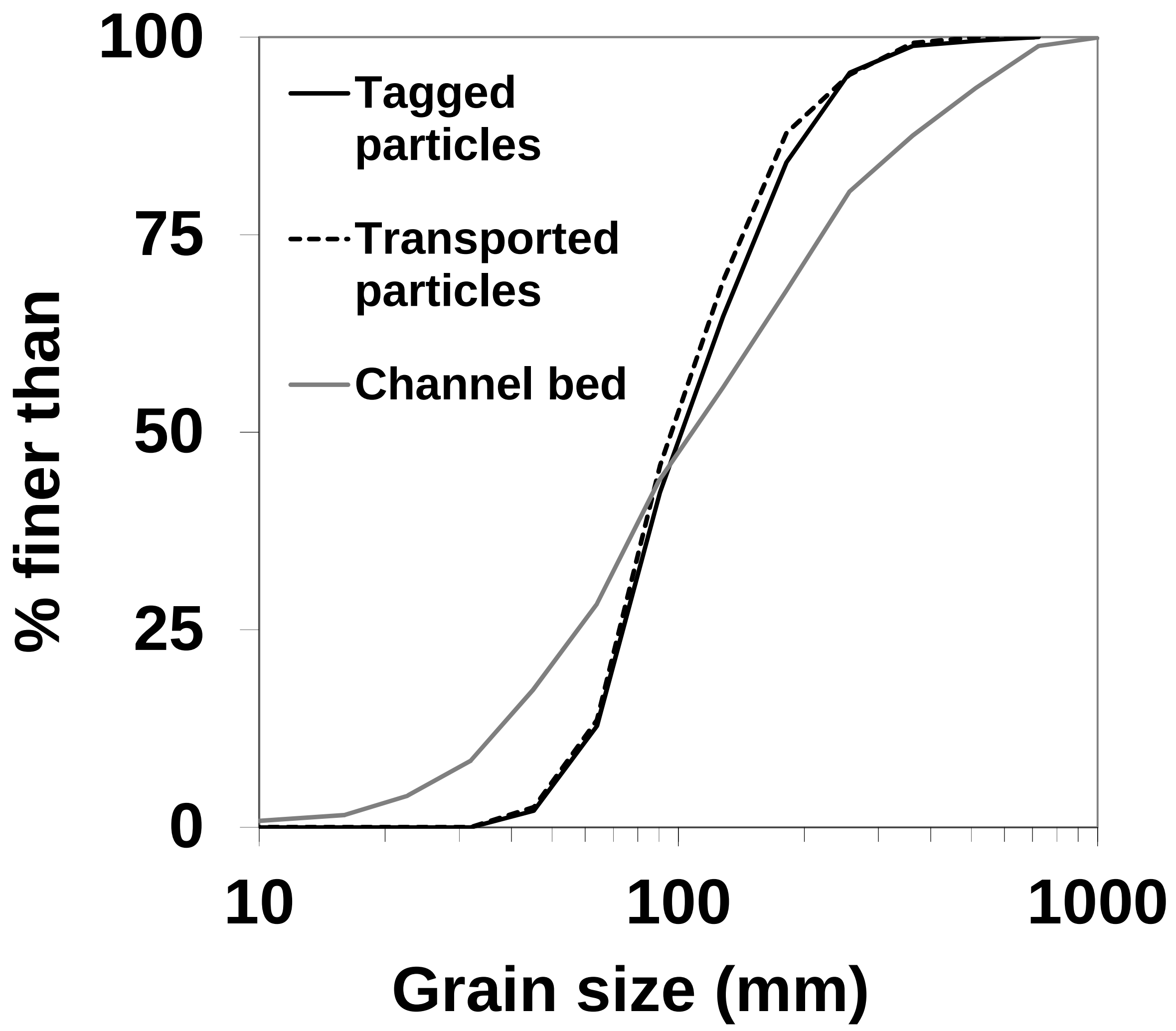

Figure (Greyscale)

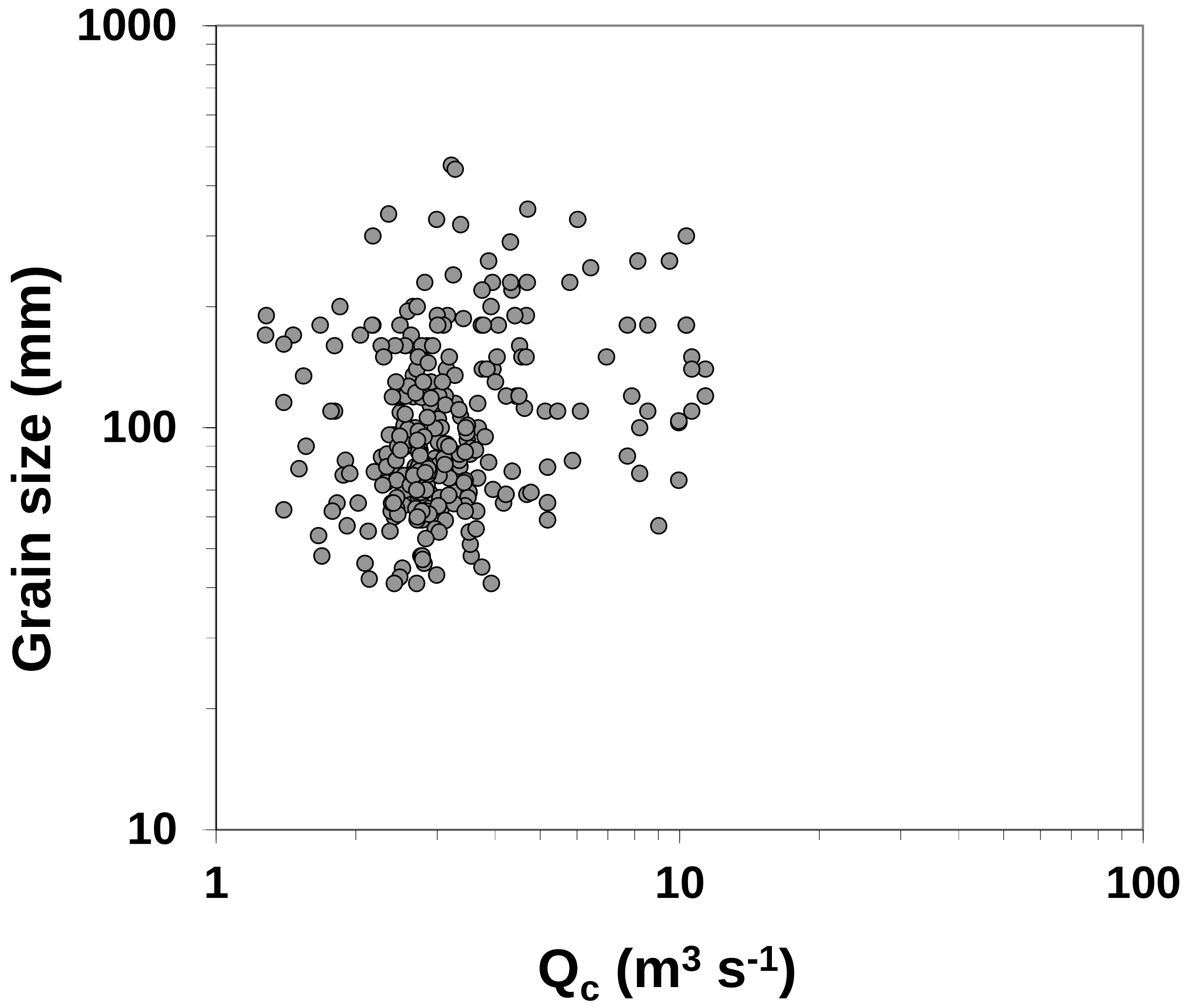

Figure (Greyscale)

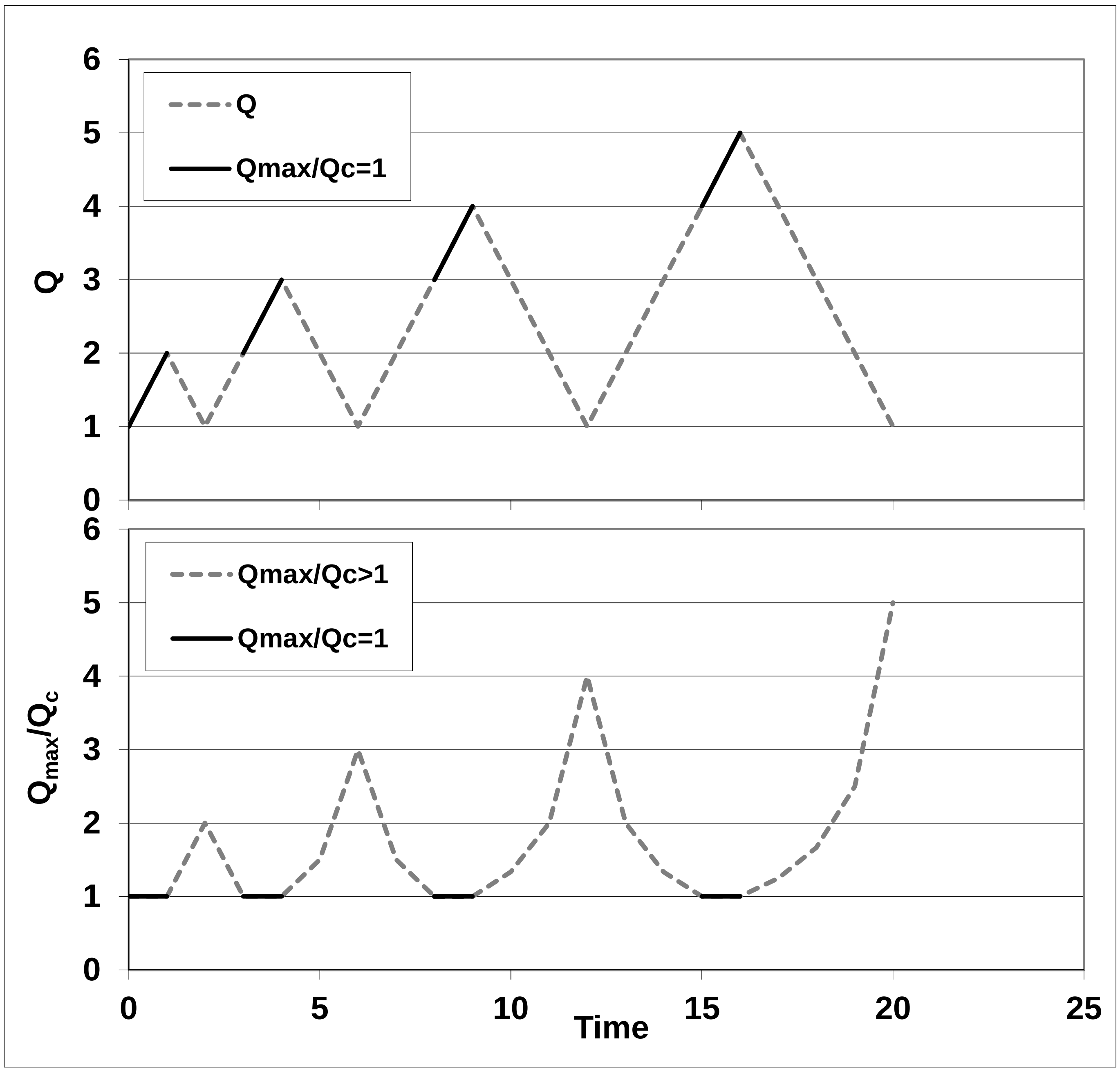

Figure (Greyscale)

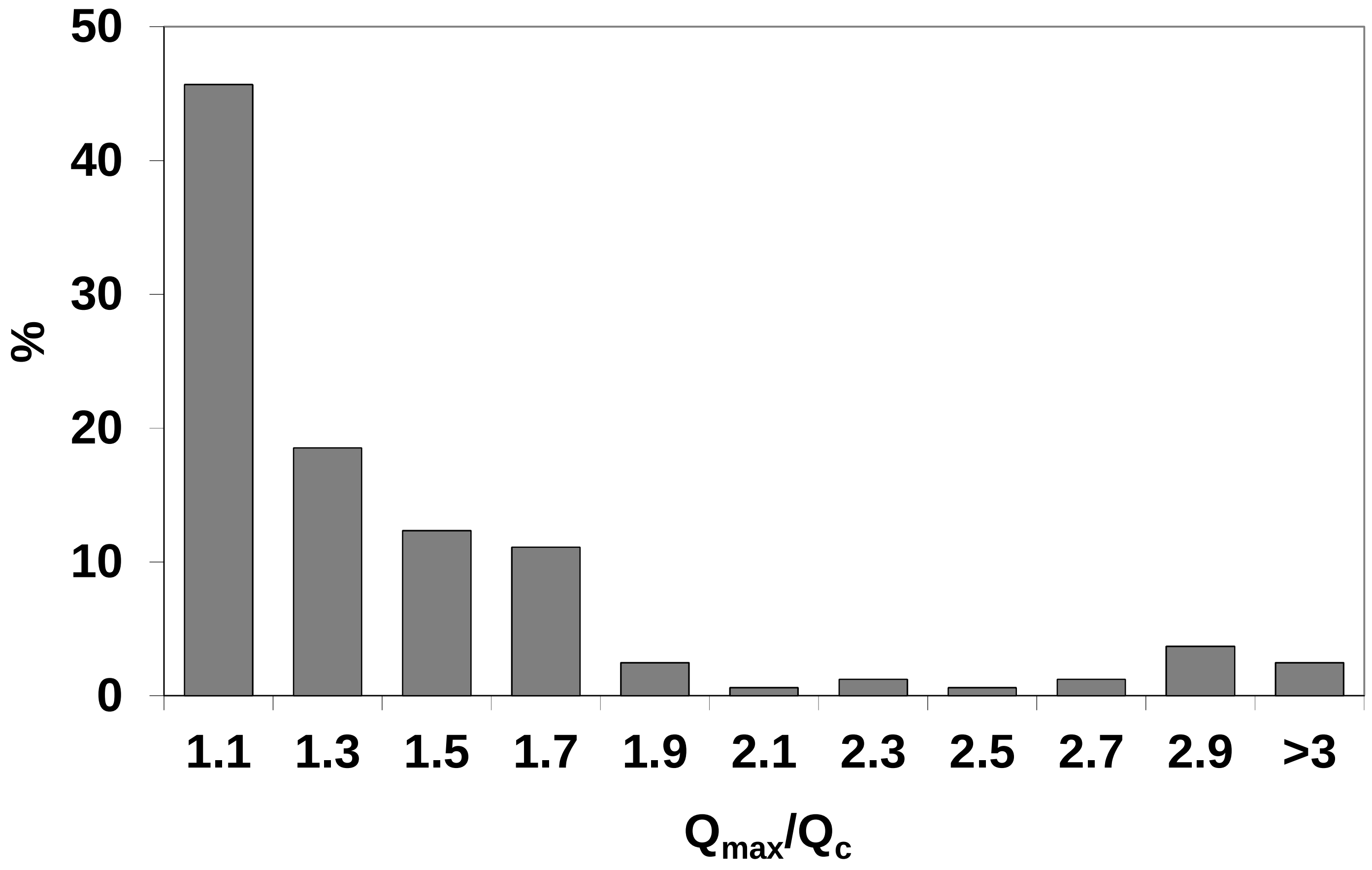

Figure (Greyscale)

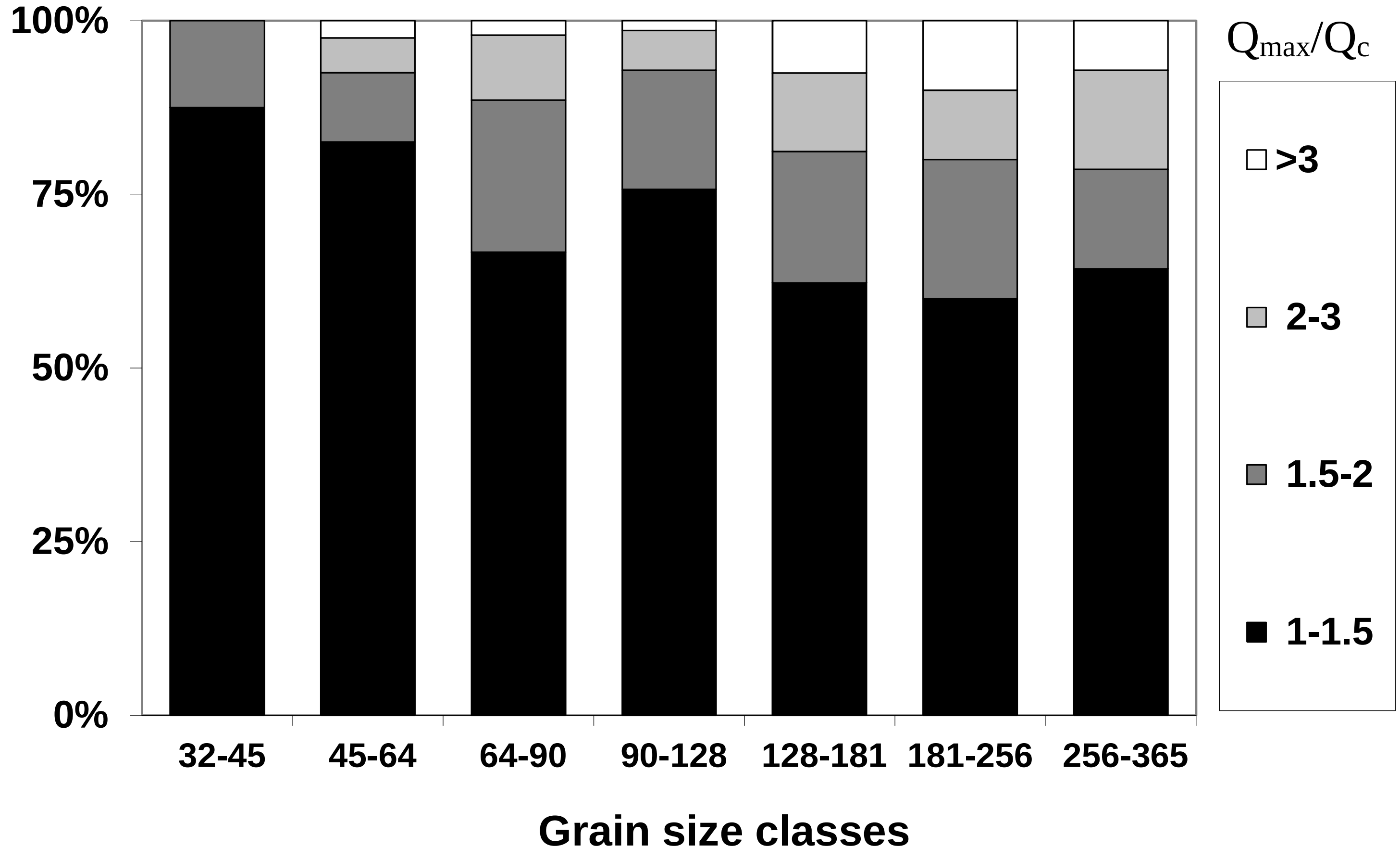

Figure (Greyscale)

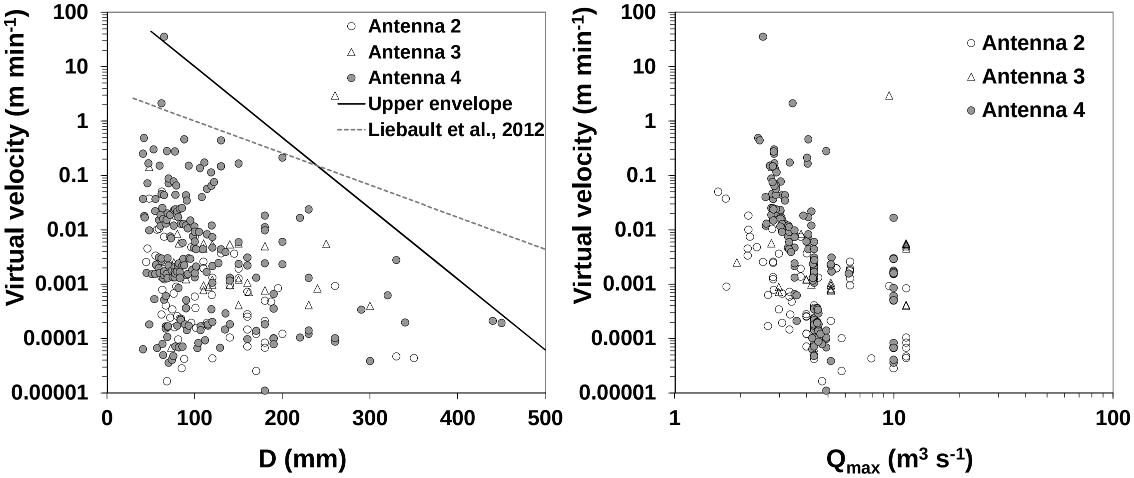

Figure (Greyscale)